



Published in final edited form as:

Neurobiol Dis. 2022 December ; 175: 105915. doi:10.1016/j.nbd.2022.105915.

Chemotherapy promotes astrocytic response to A β deposition, but not A β levels, in a mouse model of amyloid and APOE

Christi Anne S. Ng^a, Lucas P. Biran^a, Elena Galvano^a, Jeanne Mandelblatt^b, Stefano Vicini^{c,d}, G. William Rebeck^{a,d,*}

^aDepartment of Neuroscience, Georgetown University, Washington, DC, United States of America

^bDepartment of Oncology, Cancer Prevention and Control Program and Georgetown Lombardi Institute for Cancer and Aging Research, Georgetown University, Washington, DC, United States of America

^cDepartment of Pharmacology and Physiology, Georgetown University, Washington, DC, United States of America

^dInterdisciplinary Program in Neuroscience, Georgetown University, Washington, DC, United States of America

Abstract

Many cancer survivors experience cancer-related cognitive impairment (CRCI), which is characterized by problems of attention, working memory, and executive function following chemotherapy and/or hormonal treatment. APOE4, the strongest genetic risk factor for Alzheimer's Disease (AD), is also a risk factor for CRCI, especially among survivors exposed to chemotherapy. We explored whether the effects of APOE genotype to chemotherapy were associated with an increase in AD pathological processes, using a mouse model of amyloid (5XFAD) along with the E3 or E4 alleles of human APOE (E3FAD and E4FAD). Six-month-old female E3FAD mice (control $n = 5$, treated $n = 5$) and E4FAD (control $n = 6$, treated $n = 6$) were treated with two doses of doxorubicin (total 10 mg/kg) or DMSO vehicle. After six weeks, mice were euthanized and brains were analyzed by immunohistochemistry and biochemical assays. Doxorubicin-treated mice had the same level of A β in the brain as control mice, as measured by 6E10 immunohistochemistry, A β 40 and A β 42 ELISAs, and plaque morphologies. Doxorubicin significantly increased the level of the astrocytic response to A β deposits, which was independent of APOE genotype; no effects of doxorubicin were observed on the microglial responses. These data are consistent with a model in which the effects of doxorubicin on risk of CRCI are unrelated amyloid accumulation, but possibly related to glial responses to damage.

Keywords

APOE; Alzheimer's; Chemotherapy; Doxorubicin; Amyloid; Gliosis

This is an open access article under the CC BY-NC-ND license (<http://creativecommons.org/licenses/by-nc-nd/4.0/>).

*Corresponding author at: 3970 Reservoir Rd, NW, Washington, DC 20007, United States of America. gwr2@georgetown.edu (G.W. Rebeck).

1. Introduction

Cancer chemotherapy patients often experience troubling cognitive problems post-treatment, lasting from a few months to years (Eide and Feng, 2020). Preclinical and clinical studies of this cancer-related cognitive impairment (CRCI) suggest dysfunction occurs primarily in cognitive domains of memory, processing speed, and executive function (Jansen et al., 2005; Ahles et al., 2010). The brain alterations associated with chemotherapy and/or hormonal treatment involve biomarkers of aging and neurodegenerative processes (Mounier et al., 2020; Ahles et al., 2012; Sanoff et al., 2014). Interestingly, the E4 allele of the apolipoprotein E (APOE) gene, the strongest genetic risk factor for late-onset Alzheimer's disease (AD) (Ward et al., 2012; Raber et al., 2004), is also the most reproducible genetic risk factor for CRCI (Mandelblatt et al., 2018; Buskbjerg et al., 2019; Ahles et al., 2003; Fernandez et al., 2020). APOE genotype also affects normal brain function with aging, including the domains observed in CRCI (Raber et al., 2004; Flowers and Rebeck, 2020).

There are three common APOE alleles: APOE2, APOE3, and APOE4. APOE4 is found in about 25% of the US population and increases AD risk by 3–4 fold with a single allele and ~ 15 fold with two alleles, while APOE3, the most common allele, is defined as average risk (Liu et al., 2013). Female APOE4 carriers are associated with an increased risk at younger ages compared to men (Neu et al., 2017). The hallmarks of AD neuropathology are characterized by extracellular amyloid plaques, neurofibrillary tangles, and gliosis (Vinters, 2015). APOE genotype affects AD pathogenesis, including A β plaque load and glial activation (Bu, 2009; Ungar et al., 2014). In mouse models of amyloid, APOE4 is associated with increased A β levels and earlier deposition when compared with APOE3 (Tai et al., 2013; Tai et al., 2017; Youmans et al., 2012a). APOE isoforms also modulate glial activation in response to several types of damage, including amyloid, lipopolysaccharide, and acute brain injuries (Rodriguez et al., 2014; Zhu et al., 2012; Kloske and Wilcock, 2020; Ben-Moshe et al., 2020).

The success of many types of cancer treatments has allowed cancer survivorship to rise, increasing the number of individuals experiencing CRCI. Many cancer treatments induce neuroinflammation, oxidative stress, impaired neurogenesis, and peripheral damage affecting the integrity of the blood brain barrier (Fernandez et al., 2020). These CNS damages post cancer therapy share common pathways of aging and neurodegeneration (Mandelblatt et al., 2013), such as neuroinflammation, oxidative DNA damage, and decreased brain volumes (Ramassamy et al., 2000; Ahles and Saykin, 2007; McDonald et al., 2010). The shared risk of APOE4 individuals to CRCI and AD has led us to postulate that CRCI shares a causative mechanism with AD, or that cancer and its therapies are unmasking an underlying neurodegenerative process.

Both doxorubicin and APOE4 have been correlated with proinflammatory responses, such as elevated levels of cytokines and increased astroglia (Kloske and Wilcock, 2020; Cardoso et al., 2020; Overmyer et al., 1999). Previously, our group used a human APOE knock-in mouse model (APOE-TR mice) to investigate behavioral impairment post-chemotherapy in female mice and to expand on the CRCI clinical research in breast cancer patients (Mandelblatt et al., 2018; Jim et al., 2012; Bc et al., 2022). These studies demonstrated

behavioral impairments after doxorubicin treatment that recapitulate key aspects of human CRCI, including deficiencies in spatial learning and alterations in brain cortical volumes, with greater effects in APOE4 mice than in APOE3 mice (Demby et al., 2020; Speidell et al., 2019).

The APOE-TR mice do not develop the main pathological changes associated with AD, amyloid plaques and neurofibrillary tangles. Thus, we examined here the effects of chemotherapy in an established AD mouse model: EFAD mice are a cross of transgenic mice expressing five FAD mutations (5xFAD) with the APOE-TR lines. The EFAD mice demonstrate APOE-modulated phenotypes similar to human AD patients, with behavioral deficits, gliosis, A β accumulation, and synaptic protein deficits greater in E4FAD compared to E3FAD (Tai et al., 2017; Youmans et al., 2012a; Rodriguez et al., 2014; Shan et al., 2015; Balu et al., 2019). Furthermore, these mice have shown genotype specific responses to therapeutic treatments, such as RXR agonists (Tai et al., 2014) and estrogen therapy (Tai et al., 2017; Kunzler et al., 2014). Thus, EFAD mice are a good model for testing the effects of chemotherapy and other cancer therapies on AD pathological processes, incorporating the effects of APOE genotype.

In this study, we use female E4FAD and E3FAD mice to explore whether the APOE genotype-associated risk of CRCI functions through pathways of amyloid, focusing on A β aggregation and glia reactivity to plaques. We concentrated on the CRCI effects associated with chemotherapy only, absent of tumors and additional cancer-related treatments. The results are intended to contribute to identification of shared bio-logical pathways of CRCI and AD and identification of treatments and preventative approaches to improve cancer survivors' quality-of-life post-treatment.

2. Materials and methods

2.1. EFAD mice

This study was conducted in accordance with ethical standards of the Georgetown University Institutional Animal Care and Use Committee. E3FAD and E4FAD mouse lines (5xFAD^{+/-};APOE^{+/+}) were established and generously supplied by Mary Jo LaDu at the University of Illinois at Chicago. 5xFAD^{+/-} mice, a model hemizygous for 5 familial AD trans-genes (APP K670N/M671L + I716V + V717I and PS1 M146L + L286V) of C57BL/6J/B6xSJL background (Youmans et al., 2012a), were bred with APOE-TR^{+/+} mice of C57BL/6N background. The resulting APOE-TR^{+/-} / 5xFAD^{+/-} mice have been backcrossed with APOE-TR^{+/+} mice to generate the AD mouse model, hemizygous for 5xFAD and homozygous for APOE4 (E4FAD) or APOE3 (E3FAD). These mice have reproducibly demonstrated effects of APOE genotype on AD pathological and behavioral processes (Tai et al., 2017; Balu et al., 2019; M et al., 2021; Stephen et al., 2019).

Four groups of EFAD mice were used: E3FAD DMSO control ($n = 5$), E3FAD treated ($n = 5$), E4FAD DMSO control ($n = 6$), and E4FAD treated ($n = 6$). Treated mice received doxorubicin, a common chemotherapy drug. Six month old mice received two intraperitoneal injections, one week apart, of 470 μ l of sterile Phosphate-Buffered Saline (PBS) with either doxorubicin hydrochloride (Sigma) at 5 mg/kg, resulting in a total dose

of 10 mg/kg (“treated”), or 30 μ l of DMSO vehicle (“control”), as described (Demby et al., 2020). Six weeks after the last injection, mice were euthanized by CO₂ inhalation and perfused with PBS for 5 to 7 min and brains were collected. One hemisphere was dissected into cortex, hippocampus, and cerebellum then snap frozen for biochemical analyses. The other hemisphere was fixed in 4% Formalin/ 4% sucrose and transitioned through a sucrose gradient and flash frozen. The fixed hemibrains were coronally sliced at 30 μ m for immunohistochemistry.

2.2. ELISAs

A β 42, A β 40, APOE.—Snap frozen hippocampal tissue from dissected brains was homogenized in Tris Buffered Saline, pH 7.4 (TBS) then centrifuged (100,000 X g for 1 h at 4 °C). The soluble TBS fraction was collected and the pellet was resuspended in TBS with 1% Triton-X (TBS-X) and centrifuged. The TBS-X soluble fraction was then collected. The remaining pellet was resuspended in 70% Formic Acid (FA) and incubated overnight, rotating at 4 °C, and the samples centrifuged. The FA-soluble fraction was neutralized with 20 volumes of 1 M Tris base. Total protein concentrations in TBS and TBS-X fractions were measured with the Pierce BCA protein assay. Levels in TBS, TBS-X, and FA were determined using Invitrogen Human A β 42 ELISA Kit, Invitrogen Human A β 40 ELISA Kit, and Abcam Human APOE ELISA kit, per manufacturer’s instructions. For A β 42, 1 μ g of TBS and TBS-X samples were analyzed; FA samples were diluted at 1:1000. For A β 40, 9 μ g of TBS and 7 μ g of TBS-X samples were analyzed; FA samples were diluted to 1:500. For APOE, 20 μ g of TBS and TBS-X samples were analyzed; FA samples were diluted to 1:2. A two-way ANOVA with Sidak’s multiple comparison test was used to assess outcomes of measures from genotype and doxorubicin treatment.

2.3. Immunohistochemistry

6E10, Moab2, IBA1, GFAP.—The 6E10 antibody against A β /APP was used for our initial analysis of A β accumulation. Brain sections were blocked with TBS-0.25% Triton X (TBS-X) with 5% normal goat serum (NGS) blocking solution for 1.5 h. Sections were then incubated with 6E10 at a 1:1000 dilution in TBS-X with 1% NGS overnight at 4 °C. Sections were incubated with secondary antibody AlexaFluor 488 at a 1:1000 dilution in TBS-X with 1% NGS for 1 h, then incubated with DAPI at a 1:10,000 dilution.

2.4. Moab2/Iba1/GFAP

The Moab2 antibody was used as an immunostain for A β deposits (Youmans et al., 2012b). Antigen retrieval with heated citrate buffer (approximately 95 °C) was performed on sections for 3 min. Although under some conditions the Moab2 antigen is heat sensitive (Koss et al., 2016), we found antigen retrieval necessary for immunohistochemical staining. Sections were permeabilized in PBS-0.5% Triton X for 30 min and then blocked in PBS with 10% NGS and 5% bovine serum albumin for 2 h. Sections were co-stained in PBS-0.1% Tween with 1% NGS and 1% bovine serum albumin overnight at 4 °C for A β (1:1000) and either GFAP (1:2000), an astrocyte marker, or Iba1 (1:1000), a microglia marker. Slices were incubated with secondary antibodies AlexaFluor 488 at 1:1000 dilution for 1 h and AlexaFluor 594 at 1:500 for 2 h in PBS with 1% NGS.

2.5. Imaging and analysis

For 6E10 stained sections, images were captured with Zeiss Axioskop at 10× magnification. Blinded analysis with ImageJ of 6E10-positive area was performed. Images were converted to 8-bit gray scale and ROIs were drawn to outline the respective areas of CA1, CA2, CA3, and CA4 from the hippocampus and cortex layers 1, 2/3, 4, 5, 6a, and 6b. After thresholding to highlight plaques, percent area covered by 6E10 immunostain was measured.

For Moab2 stained sections, Z-stack images of the isocortex were captured using Thor Imaging Systems Division resonance laser scanning confocal microscope mounted on a Nikon Instruments upright Eclipse FN1 microscope at 60× water immersion magnification. Z-stacked images (386.55 $\mu\text{m} \times 386.55 \mu\text{m}$, 0.5 μm per stack) were converted into 2 dimensional composite images in a blinded manner using ImageJ; the number of Z-planes compressed was determined by the range in which the individual amyloid plaque appeared, which averaged 18 Z-planes.

A β plaques and Iba1 co-immunostaining was analyzed using individual fluorescent channels, red for plaques and green for microglia. Pixels were converted to microns using the following conversion scale: distance to pixels = 1, known distance = 0.337, pixel aspect ratio = 1. On the plaque channel, circular ROIs were drawn to obtain the plaque area. All non-overlapping plaques with areas completely within the composite image were selected for analysis. Plaques were subsequently categorized into three morphologies: dense core, compact, and diffuse; these classifications were determined based on categories previously described (Rodriguez et al., 2014). Dense core plaques had bright Moab2 staining with a dense center and were the largest plaques, typically with an area over 1000 μm^2 . Diffuse plaques were characterized by weaker Moab2 with wispy fibrils and no clear center. Compact plaques had bright Moab2 staining with no surrounding fibrils and were the smallest plaques with areas under 750 μm^2 . ROIs were then superimposed onto the microglial (Iba1+) channel. As a marker of microglial cell membrane, the Iba1 staining covered much of each type of plaque and demonstrated intensity differences across individual microglia. Microglia mean intensity was recorded, compensating for background intensity by subtracting the average of three background intensity recordings.

For analysis of the astrocyte-plaque interactions, A β plaques and GFAP-positive astrocytes were again visualized using individual fluorescent channels. Pixels were again converted to microns using the following conversion scale: distance to pixels = 1, known distance = 0.337, pixel aspect ratio = 1. On the A β channel, circular ROIs were drawn to obtain the plaque area, and plaque morphology was recorded. The ROIs were then superimposed on the astrocyte channel, which was then converted to 16-bit and a threshold was performed to determine the percent area coverage of the GFAP immunostaining in the plaque ROI. In contrast to intensity measurements used for Iba1 assessment, percent area coverage was used because GFAP marks only some cytoskeletal elements, without obvious differences to intensity across structures. Area was assessed within each treatment group and sorted according to the three plaque morphologies. Total plaque quantity per treatment group and percent of plaques in each morphologic group were again evaluated.

All statistical analysis was performed with GraphPadPrism 9. For all immunostaining, 2–3 images were captured within 2–3 slices per each brain. Two-way ANOVAs with Sidak's multiple comparison test were used to assess outcome measures from genotype and doxorubicin treatment of the 11 treated and 11 untreated mice, which were split between E3FAD ($n = 10$) and E4FAD ($n = 12$).

3. Results

Female E3FAD and E4FAD mice were treated at six months of age with the chemotherapeutic agent doxorubicin or vehicle. At eight months of age, the mice were euthanized and brain tissue collected. As expected for this model of amyloid (Youmans et al., 2012a), 6E10-positive plaques of various morphologies were abundantly present in the subiculum, various hippocampal subfields, and layers of the cerebral cortex (Fig. 1A).

3.1. Doxorubicin did not affect plaque accumulation

To assess the effects of chemotherapy on plaque accumulation, we measured the percent of area covered by 6E10 immunostaining in the E3FAD and E4FAD mice treated with either doxorubicin or DMSO control. No differences in plaque area were detected between doxorubicin treated and control brains in either the E3FAD or the E4FAD mice (Fig. 1B–C). We compared all E3FAD mice (treated and control) with all E4FAD mice (treated and control) in order to examine genotype differences in plaque coverage. As expected (Youmans et al., 2012a), E4FAD mice showed a higher level of plaque accumulation in the cortex than E3FAD mice (Fig. 1C, $*p = 0.039$, $**p = 0.0022$).

3.2. Hippocampal A β 42 and A β 40 levels were not affected by doxorubicin treatment

Hippocampal extraction fractions (TBS, TBS-X, and FA) were analyzed for A β 42 and A β 40 levels by ELISA (Fig. 2). A β 42 and A β 40 species were observed in each type of brain extract fraction. Consistent with A β immunostaining (Fig. 1), no significant effects of doxorubicin treatment were observed for A β 42 levels in either E3FAD or E4FAD brains in any of the three brain fractions (Fig. 2A–C).

A β 40 measures demonstrated similar results to those for A β 42. No significant effects of doxorubicin treatment were observed across the three hippocampal extraction fractions (Fig. 2D–F). E4FAD mouse brains showed higher A β 40 levels in the TBS and TBS-X fractions when compared to E3FAD mouse brains (Fig. 2D, E, $*p = 0.038$, $**p = 0.0064$). In addition, no differences in levels of apoE protein were observed in any fraction across APOE genotypes or treatments (data not shown).

3.3. Doxorubicin did not affect plaque morphology or quantity in the isocortex

To examine whether doxorubicin affected specific plaque types, we used the anti-A β antibody Moab2, and analyzed the types of over 1000 amyloid plaques present in the isocortex (Fig. 3). There were no significant effects of doxorubicin in either the E3FAD or E4FAD mice. Overall, E4FADs (treated and control) showed more plaque deposition compared to E3FADs (Fig. 3D, $*p = 0.016$), consistent with the results of the 6E10 percent area coverage analysis. Then we defined individual amyloid plaques as diffuse (Fig. 3A),

dense core (Fig. 3B), or compact (Fig. 3C), and calculated each plaque morphology as a percent of the total plaque numbers (Fig. 3E–K). Doxorubicin showed no impact on plaques of different morphology types. E4FAD controls had more of the diffuse plaques when compared with E3FAD controls (Fig. 3E, # $p = 0.041$), while the percentage of compact plaques was lower (Fig. 3G, ## $p = 0.0009$). E4FADs (treated and control) showed higher levels of dense core plaques and a lower number of compact plaques compared to E3FADs (Fig. 3F&G, ** $p = 0.0023$, *** $p = 0.0004$). Thus, there are distribution differences of plaque types by APOE genotype, but without an effect of doxorubicin treatment (Fig. 3H–K).

3.4. Doxorubicin did not impact microglial reactivity to plaques

To test whether chemotherapy affected the microglial response to A β plaques, we assessed microglial activation within the area of over 500 individual plaques using co-immunofluorescence of Moab2 and Iba1 in the isocortex (Fig. 4A). We drew circular ROIs to establish the areas affected by individual plaques (Fig. 4B), then separated the fluorescent channels in order to measure the fluorescence intensity of the Iba1 positive cells within the ROIs (Fig. 4C). This approach allowed us to determine whether there were differences in microglial responses to individual plaques as compared to whether the brain as a whole had more microglia. Through quantification of microglia intensity per plaque area, we saw no effects of doxorubicin on microglia reactivity in either E3FAD or E4FAD brains (Fig. 4D). Next, we assessed whether microglia responded differently to plaques of the various morphologies (Fig. 4E–G). No effects of doxorubicin were seen around dense core, diffuse, or compact plaques. Microglial intensity around diffuse plaques was significantly higher in control brains of E4FAD mice compared to E3FAD mice (# $p = 0.04$).

3.5. Doxorubicin increased astrocytic reactivity to dense core and compact plaques

We next investigated the astrocytic response to A β plaques after doxorubicin exposure. Using isocortex tissue double stained with Moab2 and GFAP (Fig. 5A), we measured the percent area of over 500 individual plaques occupied by GFAP immunostaining. No impact of doxorubicin treatment was seen in E3FAD or E4FAD mice toward plaques overall (Fig. 5D). However, doxorubicin treatment significantly increased the astrocytic response to both dense core and compact plaques, controlling for APOE genotype ($p = 0.036$, \$\$ $p = 0.016$, respectively). Individually, doxorubicin in E3FAD mice induced significantly greater astrocyte coverage of dense core plaques compared to control conditions (## $p = 0.0081$), but there were no significant effects in E4FAD mice. In control brains, there was a significantly stronger astrocytic response to both dense core and diffuse plaques in E4FAD mice compared to E3FAD mice (### $p = 0.0025$, # $p = 0.013$). Finally, there was a stronger astrocytic response to diffuse plaques of E4FAD mice compared to E3FAD mice across treatment conditions (* $p = 0.0009$).

4. Discussion

Clinical research suggests that cancer-related cognitive impairment (CRCI) has many parallels with accelerated processes of aging and with Alzheimer's disease (AD) risk factors, including the genetic factor APOE4 (Ahles et al., 2003; Fernandez et al., 2020; Mandelblatt et al., 2013; Mandelblatt et al., 2014). We previously found that, consistent with human

studies, exposure to the chemotherapy doxorubicin had greater behavioral effects on APOE4 mice compared to APOE3 mice (Demby et al., 2020; Speidell et al., 2019). In the current study, we tested whether doxorubicin treatment could directly impact AD pathology, using an amyloid mouse model that incorporates the human APOE alleles (EFAD). We found that doxorubicin treatment did not increase A β accumulation, as measured by several immunohistochemical and biochemical assays. Doxorubicin did significantly increase the astrocytic response to the two more mature types of A β deposits, dense core plaques and compact plaques. Although we were testing how chemotherapy affected AD pathogenesis related to APOE genotype, this observed effect was independent of APOE genotype. These results could suggest that the APOE4 risk for CRCI is related to CNS alterations, but that effects may not involve amyloid pathways.

Amyloid accumulation is the earliest known biomarker of AD pathological changes (Zetterberg and Bendlin, 2021). It is observed through PET scans or changes to CSF A β 42 levels up to two decades before the accumulation of neurofibrillary tangles or the overt clinical symptoms of dementia (Sanchez et al., 2021). We used a mouse model of A β accumulation because we reasoned that effects of chemotherapy would be on individuals with early amyloid accumulation but without the clinical signs of AD. The preclinical model of EFAD mice allows detection of early A β accumulation between two to six months of age across APOE genotypes (Youmans et al., 2012a); this level continues to increase to at least 18 months of age (Balu et al., 2019). We exposed EFAD mice to doxorubicin at six months of age and examined their brains at eight months of age. Since this mouse model allows A β accumulations over a long period of time, these experiments tested whether doxorubicin promoted growth of existing deposits and the development of new deposits.

Abnormal levels and ratios of amyloid beta peptides is a common hallmark of AD, with amyloid plaques consisting mostly of A β 42 (Qiu et al., 2015). Using immunostains for total A β or A β 42 and ELISAs for A β 40 and A β 42, we saw no effects of doxorubicin chemotherapy on A β levels. One limitation of this work is that we analyzed mice at a single stage of A β accumulation. Additional experiments in models of slower amyloid accumulation could test whether doxorubicin influences initial accumulation of amyloid, or has effects if administered over longer periods of time. However, if our current mouse work is replicated, it would imply that individuals being treated with doxorubicin for cancer might not be at greater risk of AD-associated amyloid.

In addition to CRCI, APOE4 genotype is associated with the progression of other CNS conditions that do not include A β accumulation. APOE4 is associated with an increased risk of Lewy Body Dementia (Chia et al., 2021), greater α -synuclein accumulation (Zhao et al., 2020), and a decreased age of onset of this disease (Schaffert et al., 2020). APOE4 is also associated with increased brain atrophy and behavioral impairment in Frontotemporal Dementia (Agosta et al., 2009; Engelborghs et al., 2006). In addition to neurodegenerative conditions, APOE4 may predispose to CNS phenotypes after infection with covid-19 (Kuo et al., 2022) or chronic CNS HIV infection (Yang et al., 2021). These CNS phenotypes of viral infections induce brain dysfunction with somewhat variable and poorly defined cognitive problems that may share other APOE-driven susceptibilities with CRCI. Together,

these studies support the hypothesis that APOE4 could affect cognitive impairment in many conditions via a mechanism that does not involve A β accumulation.

One pathological process that is common to these APOE4-related impairments is chronic inflammation. Neuroinflammation is associated with both causing and exacerbating cognitive impairment during neurodegenerative diseases and brain injury (Lyman et al., 2014), regulated by astrocytic and microglial proliferation in order to repair damage and phagocytose debris (Guzman-Martinez et al., 2019). APOE is mainly produced by glial cells, with APOE4 associated with fostering pro-inflammatory environments including increased activation of microglia and astrocytes (Kloske and Wilcock, 2020; Rebeck, 2017). Our current study generally validated our earlier findings that mice expressing APOE4 had significantly greater glial responses to individual plaques than mice expressing APOE3 (Rodriguez et al., 2014); this effect was found for the microglial response to diffuse plaques and the astrocytic response to dense core and diffuse plaques. Previous work showed that APOE4 had a different effect on microglial response toward Thioflavin S-positive compact plaques (Stephen et al., 2019), perhaps relating to plaque maturity. The effect of APOE genotype on inflammation has fostered several therapies, including mimetic peptides and APOE-related molecules to promote cholesterol efflux (Lanfranco et al., 2020).

Cancer chemotherapy promotes peripheral inflammation as well as signs of CNS inflammation (Fernandez et al., 2020). For example, rodent studies show that chemotherapy treatments increase brain TNF α and IL-6 levels and astrogliosis (Cardoso et al., 2020; Tangpong et al., 2006). Many chemotherapeutic agents, including doxorubicin, do not cross the blood brain barrier, but may trigger peripheral inflammatory mediators, such as cytokines, that can penetrate the blood brain barrier and promote proliferation of glial cells within the brain (Fernandez et al., 2020; Ren, and St. Clair DK, Butterfield DA., 2017). Controlling for APOE genotype, we found that doxorubicin increased astrocytic reactivity to dense core and compact plaques (but not diffuse plaques). Glial activation is one of the original defining aspects of the AD pathological changes (Alzheimer et al., 1995). Recent AD genetics (Podl \acute{e} сны-Drabiniok et al., 2020) and detailed neuropathological analyses (Perez-Nievas et al., 2013; Haage and De Jager, 2022) support the hypothesis that inflammation may contribute to risk of the onset of AD and to the progression to cognitive impairment. There may be CNS astrocytic pathways promoted by chemotherapy in response to the denser A β accumulations.

The observed effects of doxorubicin on astrocytic activation (GFAP immunostaining) represent one aspect of the inflammatory cascades. Although GFAP is a commonly used cytoskeletal marker and considered a hallmark of reactive astrocytes, it only labels a mature subpopulation of astrocytes where intermediate filament protein is present (Preston et al., 2019). Multiple signaling pathways activate and modulate pro-inflammatory astrocytes, including the JAK-STAT3 pathway that initiates reactive astrocytes and the NF- κ B pathway (Kwon and Koh, 2020; Giovannoni and Quintana, 2020; Linnerbauer et al., 2020); the effects of doxorubicin on these pathways should be investigated. Given the heterogenous nature of inflammatory processes, broad approaches into mechanisms independent of A β would be important to test hypotheses related to doxorubicin exposure and neuroinflammation.

There are several limitations to be considered before determining the impact of our conclusions, including small sample numbers (11 untreated and 11 treated mice, split between the two APOE genotypes). We used only female mice because, as a model of breast cancer treatment, our previous work on mouse behavior was limited to female mice; it will be important to include sex as a variable in future studies, because sex affects behavior, pathology (Tai et al., 2017) and microglial responses to amyloid (Stephen et al., 2019; Amidi et al., 2017). We also focused on the effects of a single chemotherapeutic agent, doxorubicin, in tumor-naïve mice; it will be important in future experiments to investigate the impacts of additional treatments and of the cancer itself.

Finally, these mice were susceptible to amyloid pathology only. We did not look at mice absent of AD pathology nor mice susceptible to other major neuropathological hallmarks of AD, such as neurofibrillary tangles. APOE expression predisposed to tau spreading in human brains as correlated in tau PET analysis and transcriptome measures (Montal et al., 2022). There are appropriate mouse models to test whether chemotherapy increases tau accumulation with overexpression of mutant tau in the presence of APOE3 or APOE4. These models show adverse effects of APOE4 on tau phosphorylation and misfolding (Jablonski et al., 2021), on tau propagation (Williams et al., 2022), and on brain atrophy and neurodegeneration (Shi et al., 2017). Analyses of these models could test whether chemotherapy affected tau accumulation in an APOE-dependent manner, as we have done here for A β .

The cognitive impairment seen associated with cancer and its treatments has driven studies into whether cancer increases the risk of AD. A meta-analysis of published cohort studies and case-controls studies found that cancer was associated with lower chance of AD (Ospina-Romero et al., 2020). Cancer was also associated with lower levels of AD pathological changes related to tau accumulation (Yarchoan et al., 2017; Karanth et al., 2022), further supporting some protective aspect of cancer toward AD. However, these studies did leave open the possibility that treatments for cancer might increase risk of AD (Okereke and Meadows, 2019), a hypothesis that we have only begun to examine in preclinical models here.

5. Conclusions

Our current work showed no evidence that the chemotherapeutic drug doxorubicin promoted early markers of AD pathogenesis in a mouse model of amyloidogenesis: it did not increase levels of soluble or insoluble forms of A β , nor did it affect the distribution of types of A β deposits. However, doxorubicin did increase the astrocytic response to the dense core and compact forms of A β deposits. These findings suggest future investigation of susceptibility to CRCI requires exploration in aspects of cognitive dysfunction beyond amyloid accumulation and the importance of continuing the investigation of other aspects of the inflammatory cascade.

Acknowledgements

The authors are grateful to MaryJo LaDu for providing the EFAD mice used in this study. This work was supported by National Institute of Aging at the National Institutes of Health, grant R01AG067258, and the National

Institute of Neurological Disorders and Stroke at the National Institutes of Health, grant R01NS100704 (GWR). The research was also supported by National Cancer Institute of the National Institutes of Health through grants R01CA129769 and R35CA197289 (JM).

Data availability

Data will be made available on request.

Abbreviations:

AD	Alzheimer's Disease
APOE	Apolipoprotein E
APOE-TR	APOE Targeted Replacement mice
CNS	Central Nervous System
CRCI	Cancer Related Cognitive Impairment
EFAD	APOE Familial Alzheimer's Disease mouse model
FA	Formic Acid
GFAP	Glial Fibrillary Acidic Protein
Iba1	Ionized calcium binding adaptor molecule 1
PBS	Phosphate-Buffered Saline
ROI	Region of Interest
TBS	Tris-Buffered Saline
TBS-X	Tris-Buffered Saline with Triton X

References

- Agosta F, Vessel KA, Miller BL, Migliaccio R, Bonasera SJ, Filippi M, et al. , 2009 Feb 10. Apolipoprotein E epsilon4 is associated with disease-specific effects on brain atrophy in Alzheimer's disease and frontotemporal dementia. *Proc. Natl. Acad. Sci. U. S. A* 106 (6), 2018–2022. [PubMed: 19164761]
- Ahles TA, Saykin AJ, 2007 Mar. Candidate mechanisms for chemotherapy-induced cognitive changes. *Nat. Rev. Cancer* 7 (3), 192–201. [PubMed: 17318212]
- Ahles TA, Saykin AJ, Noll WW, Furstenberg CT, Guerin S, Cole B, et al. , 2003 Sep. The relationship of APOE genotype to neuropsychological performance in long-term cancer survivors treated with standard dose chemotherapy. *Psychooncology* 12 (6), 612–619. [PubMed: 12923801]
- Ahles TA, Saykin AJ, McDonald BC, Li Y, Furstenberg CT, Hanscom BS, et al. , 2010 Oct 10. Longitudinal assessment of cognitive changes associated with adjuvant treatment for breast cancer: impact of age and cognitive reserve. *J. Clin. Oncol* 28 (29), 4434–4440. [PubMed: 20837957]
- Ahles TA, Root JC, Ryan EL, 2012 Oct 20. Cancer- and cancer treatment-associated cognitive change: an update on the state of the science. *J. Clin. Oncol* 30 (30), 3675–3686. [PubMed: 23008308]
- Alzheimer A, Stelzmann RA, Schnitzlein HN, Murtagh FR, 1995. An English translation of Alzheimer's 1907 paper, "Über eine eigenartige Erkrankung der Hirnrinde". *Clin. Anat* 8 (6), 429–431. [PubMed: 8713166]

- Amidi A, Agerbæk M, Wu LM, Pedersen AD, Mehlsen M, Clausen CR, et al. , 2017 Jun. Changes in cognitive functions and cerebral grey matter and their associations with inflammatory markers, endocrine markers, and APOE genotypes in testicular cancer patients undergoing treatment. *Brain Imaging Behav* 11 (3), 769–783. [PubMed: 27240852]
- Balu D, Karstens AJ, Loukenas E, Maldonado Weng J, York JM, Valencia-Olvera AC, et al. , 2019 Aug. The role of APOE in transgenic mouse models of AD. *Neurosci. Lett* 10 (707), 134285.
- Bc M, Vd K, Ri D, Jn B, Wa Z, Je C, et al. , 2022 Jul. Multimodal MRI examination of structural and functional brain changes in older women with breast cancer in the first year of antiestrogen hormonal therapy. *Breast Cancer Res. Treatment* [Internet] 194 (1) [cited 2022 Oct 6]. Available from: <https://pubmed.ncbi.nlm.nih.gov/35476252/>.
- Ben-Moshe H, Luz I, Liraz O, Boehm-Cagan A, Salomon-Zimri S, Michaelson D, 2020 Jan. ApoE4 exacerbates hippocampal pathology following acute brain penetration injury in female mice. *J. Mol. Neurosci* 70 (1), 32–44. [PubMed: 31489583]
- Bu G, 2009 May. Apolipoprotein E and its receptors in Alzheimer’s disease: pathways, pathogenesis and therapy. *Nat. Rev. Neurosci* 10 (5), 333–344. [PubMed: 19339974]
- Buskbjerg CDR, Amidi A, Demontis D, Nissen ER, Zachariae R, 2019 May. Genetic risk factors for cancer-related cognitive impairment: a systematic review. *Acta Oncol* 58 (5), 537–547. [PubMed: 30822178]
- Cardoso CV, de Barros MP, Bachi ALL, Bernardi MM, Kirsten TB, de Fátima Monteiro Martins M, et al. , 2020 Jan. Chemobrain in rats: behavioral, morphological, oxidative and inflammatory effects of doxorubicin administration. *Behav. Brain Res* 27 (378), 112233.
- Chia R, Sabir MS, Bandres-Ciga S, Saez-Atienzar S, Reynolds RH, Gustavsson E, et al. , 2021 Mar. Genome sequencing analysis identifies new loci associated with Lewy body dementia and provides insights into its genetic architecture. *Nat. Genet* 53 (3), 294–303. [PubMed: 33589841]
- Demby TC, Rodriguez O, McCarthy CW, Lee YC, Albanese C, Mandelblatt J, et al. , 2020 Apr. A mouse model of chemotherapy-related cognitive impairments integrating the risk factors of aging and APOE4 genotype. *Behav. Brain Res* 20 (384), 112534.
- Eide S, Feng ZP, 2020 Aug. Doxorubicin chemotherapy-induced “chemo-brain”: Meta-analysis. *Eur. J. Pharmacol* 15 (881), 173078.
- Engelborghs S, Dermaut B, Mariën P, Symons A, Vloeberghs E, Maertens K, et al. , 2006 Feb. Dose dependent effect of APOE epsilon4 on behavioral symptoms in frontal lobe dementia. *Neurobiol. Aging* 27 (2), 285–292. [PubMed: 16399213]
- Fernandez HR, Varma A, Flowers SA, Rebeck GW, 2020 Dec 19. Cancer chemotherapy related cognitive impairment and the impact of the Alzheimer’s disease risk factor APOE. *Cancers (Basel)* 12 (12), E3842.
- Flowers SA, Rebeck GW, 2020 Mar. APOE in the Normal brain. *Neurobiol. Dis* 136, 104724. [PubMed: 31911114]
- Giovannoni F, Quintana FJ, 2020 Sep. The role of astrocytes in CNS inflammation. *Trends Immunol* 41 (9), 805–819. [PubMed: 32800705]
- Guzman-Martinez L, Maccioni RB, Andrade V, Navarrete LP, Pastor MG, RamosEscobar N, 2019 Sep. Neuroinflammation as a common feature of neurodegenerative disorders. *Front. Pharmacol* 12 (10), 1008.
- Haage V, De Jager PL, 2022 Jun. Neuroimmune contributions to Alzheimer’s disease: a focus on human data. *Mol. Psychiatry*, 35668160. 10.1038/s41380-022-01637-0.
- Jablonski AM, Warren L, Usenovic M, Zhou H, Sugam J, Parmentier-Batteur S, et al. , 2021 Feb 9. Astrocytic expression of the Alzheimer’s disease risk allele, ApoEε4, potentiates neuronal tau pathology in multiple preclinical models. *Sci. Rep* 11 (1), 3438. [PubMed: 33564035]
- Jansen CE, Miaskowski C, Dodd M, Dowling G, Kramer J, 2005 Nov 15. A metaanalysis of studies of the effects of cancer chemotherapy on various domains of cognitive function. *Cancer* 104 (10), 2222–2233. [PubMed: 16206292]
- Jim HSL, Phillips KM, Chait S, Faul LA, Popa MA, Lee YH, et al. , 2012 Oct 10. Meta-analysis of cognitive functioning in breast cancer survivors previously treated with standard-dose chemotherapy. *J. Clin. Oncol* 30 (29), 3578–3587. [PubMed: 22927526]

- Karant SD, Katsumata Y, Nelson PT, Fardo DW, McDowell JK, Schmitt FA, et al. , 2022 Jul 1. Cancer diagnosis is associated with a lower burden of dementia and less Alzheimer's-type neuropathology. *Brain* 145 (7), 2518–2527. [PubMed: 35094057]
- Kloske CM, Wilcock DM, 2020. The important Interface between apolipoprotein E and Neuroinflammation in Alzheimer's disease. *Front. Immunol* 11, 754. [PubMed: 32425941]
- Koss DJ, Jones G, Cranston A, Gardner H, Kanaan NM, Platt B, 2016. Soluble pre-fibrillar tau and β -amyloid species emerge in early human Alzheimer's disease and track disease progression and cognitive decline. *Acta Neuropathol* 132 (6), 875–895. [PubMed: 27770234]
- Kunzler J, Youmans KL, Yu C, Ladu MJ, Tai LM, 2014 Feb. APOE modulates the effect of estrogen therapy on A β accumulation EFAD-Tg mice. *Neurosci. Lett* 7 (560), 131–136.
- Kuo CL, Pilling LC, Atkins JL, Fortinsky RH, Kuchel GA, Melzer D, 2022 Apr 1. APOE e4 genotypes increase risk of delirium during COVID-19-related hospitalizations: evidence from a large UK cohort. *J. Gerontol. A Biol. Sci. Med. Sci* 77 (4), 879–880. [PubMed: 34171089]
- Kwon HS, Koh SH, 2020 Nov 26. Neuroinflammation in neurodegenerative disorders: the roles of microglia and astrocytes. *Transl. Neurodegener* 9 (1), 42. [PubMed: 33239064]
- Lanfranco MF, Ng CA, Rebeck GW, 2020 Sep 1. ApoE Lipidation as a therapeutic target in Alzheimer's disease. *Int. J. Mol. Sci* 21 (17), E6336.
- Linnerbauer M, Wheeler MA, Quintana FJ, 2020 Nov 25. Astrocyte crosstalk in CNS inflammation. *Neuron* 108 (4), 608–622. [PubMed: 32898475]
- Liu CC, Liu CC, Kanekiyo T, Xu H, Bu G, 2013 Feb. Apolipoprotein E and Alzheimer disease: risk, mechanisms and therapy. *Nat. Rev. Neurol* 9 (2), 106–118. [PubMed: 23296339]
- Lyman M, Lloyd DG, Ji X, Vizcaychipi MP, Ma D, 2014 Feb. Neuroinflammation: the role and consequences. *Neurosci. Res* 1 (79), 1–12.
- M C, Te M, Ce F, 2021 Jul. Age, sex, and cerebral microbleeds in EFAD Alzheimer disease mice. *Neurobiol. Aging* [Internet] 103 [cited 2022 Oct 17]. Available from: <https://pubmed.ncbi.nlm.nih.gov/33813349/>.
- Mandelblatt JS, Hurria A, McDonald BC, Saykin AJ, Stern RA, VanMeter JW, et al. , 2013 Dec. Cognitive effects of cancer and its treatments at the intersection of aging: what do we know; what do we need to know? *Semin. Oncol* 40 (6), 709–725. [PubMed: 24331192]
- Mandelblatt JS, Stern RA, Luta G, McGuckin M, Clapp JD, Hurria A, et al. , 2014 Jun 20. Cognitive impairment in older patients with breast cancer before systemic therapy: is there an interaction between cancer and comorbidity? *J. Clin. Oncol* 32 (18), 1909–1918. [PubMed: 24841981]
- Mandelblatt JS, Small BJ, Luta G, Hurria A, Jim H, McDonald BC, et al. , 2018 Oct 3. Cancer-related cognitive outcomes among older breast Cancer survivors in the thinking and living with Cancer study. *J. Clin. Oncol* 36 (32), 3211–3222. JCO1800140.
- McDonald BC, Conroy SK, Ahles TA, West JD, Saykin AJ, 2010 Oct. Gray matter reduction associated with systemic chemotherapy for breast cancer: a prospective MRI study. *Breast Cancer Res. Treat* 123 (3), 819–828. [PubMed: 20690040]
- Montal V, Diez I, Kim CM, Orwig W, Bueichekú E, Gutiérrez-Zúñiga R, et al. , 2022 Jul 27. Network tau spreading is vulnerable to the expression gradients of APOE and glutamatergic-related genes. *Sci. Transl. Med* 14 (655), eabn7273.
- Mounier NM, Abdel-Maged AES, Wahdan SA, Gad AM, Azab SS, 2020 Oct. Chemotherapy-induced cognitive impairment (CICI): an overview of etiology and pathogenesis. *Life Sci* 1 (258), 118071.
- Neu SC, Pa J, Kukull W, Beekly D, Kuzma A, Gangadharan P, et al. , 2017 Oct 1. Apolipoprotein E genotype and sex risk factors for Alzheimer's disease. *JAMA Neurol* 74 (10), 1178–1189. [PubMed: 28846757]
- Okereke OI, Meadows ME, 2019 Jun 5. More evidence of an inverse association between Cancer and Alzheimer disease. *JAMA Netw. Open* 2 (6), e196167. [PubMed: 31225887]
- Ospina-Romero M, Glymour MM, Hayes-Larson E, Mayeda ER, Graff RE, Brenowitz WD, et al. , 2020 Nov 2. Association between Alzheimer disease and Cancer with evaluation of study biases: a systematic review and Meta-analysis. *JAMA Netw. Open* 3 (11), e2025515. [PubMed: 33185677]
- Overmyer M, Helisalmi S, Soininen H, Laakso M, Riekkinen P, Alafuzoff I, 1999 Aug. Astrogliosis and the ApoE genotype. An immunohistochemical study of postmortem human brain tissue. *Dement. Geriatr. Cogn. Disord* 10 (4), 252–257. [PubMed: 10364641]

- Perez-Nievas BG, Stein TD, Tai HC, Dols-Icardo O, Scotton TC, Barroeta-Espar I, et al. , 2013 Aug. Dissecting phenotypic traits linked to human resilience to Alzheimer's pathology. *Brain* 136 (Pt 8), 2510–2526. [PubMed: 23824488]
- Podl\'esny-Drabiniok A, Marcora E, Goate AM, 2020 Dec. Microglial phagocytosis: a disease-associated process emerging from Alzheimer's disease genetics. *Trends Neurosci* 43 (12), 965–979. [PubMed: 33127097]
- Preston AN, Cervasio DA, Laughlin ST, 2019. Visualizing the brain's astrocytes. *Methods Enzymol* 622, 129–151. [PubMed: 31155050]
- Qiu T, Liu Q, Chen YX, Zhao YF, Li YM, 2015 Jul. A β 42 and A β 40: similarities and differences. *J. Pept. Sci* 21 (7), 522–529. [PubMed: 26018760]
- Raber J, Huang Y, Ashford JW, 2004 Jun. ApoE genotype accounts for the vast majority of AD risk and AD pathology. *Neurobiol. Aging* 25 (5), 641–650. [PubMed: 15172743]
- Ramassamy C, Averill D, Beffert U, Theroux L, Lussier-Cacan S, Cohn JS, et al. , 2000 Feb. Oxidative insults are associated with apolipoprotein E genotype in Alzheimer's disease brain. *Neurobiol. Dis* 7 (1), 23–37. [PubMed: 10671320]
- Rebeck GW, 2017 Aug. The role of APOE on lipid homeostasis and inflammation in normal brains. *J. Lipid Res* 58 (8), 1493–1499. [PubMed: 28258087]
- Ren X, St. Clair DK, Butterfield DA., 2017 Mar. Dysregulation of cytokine mediated chemotherapy induced cognitive impairment. *Pharmacol. Res* 1 (117), 267–273.
- Rodriguez GA, Tai LM, LaDu MJ, Rebeck GW, 2014 Jun. Human APOE4 increases microglia reactivity at A β plaques in a mouse model of A β deposition. *J. Neuroinflammation* 19 (11), 111.
- Sanchez JS, Hanseeuw BJ, Lopera F, Sperling RA, Baena A, Bocanegra Y, et al. , 2021 Jan 15. Longitudinal amyloid and tau accumulation in autosomal dominant Alzheimer's disease: findings from the Colombia-Boston (COLBOS) biomarker study. *Alzheimers Res. Ther* 13 (1), 27. [PubMed: 33451357]
- Sanoff HK, Deal AM, Krishnamurthy J, Torrice C, Dillon P, Sorrentino J, et al. , 2014 Apr. Effect of cytotoxic chemotherapy on markers of molecular age in patients with breast cancer. *J. Natl. Cancer Inst* 106 (4), dju057.
- Schaffert J, LoBue C, White CL, Wilmoth K, Didehban N, Lacritz L, et al. , 2020 Mar. Risk factors for earlier dementia onset in autopsy-confirmed Alzheimer's disease, mixed Alzheimer's with Lewy bodies, and pure Lewy body disease. *Alzheimers Dement* 16 (3), 524–530. [PubMed: 32043803]
- Shan Liu D., Dong Pan X., Zhang J, Shen H, Collins NC, Cole AM, et al. , 2015 Mar. APOE4 enhances age-dependent decline in cognitive function by down-regulating an NMDA receptor pathway in EFAD-Tg mice. *Mol. Neurodegener* 5 (10), 7.
- Shi Y, Yamada K, Liddelow SA, Smith ST, Zhao L, Luo W, et al. , 2017 Sep 28. ApoE4 markedly exacerbates tau-mediated neurodegeneration in a mouse model of tauopathy. *Nature* 549 (7673), 523–527. [PubMed: 28959956]
- Speidell AP, Demby T, Lee Y, Rodriguez O, Albanese C, Mandelblatt J, et al. , 2019 Feb. Development of a human APOE knock-in mouse model for study of cognitive function after cancer chemotherapy. *Neurotox. Res* 35 (2), 291–303. [PubMed: 30284204]
- Stephen TL, Cacciottolo M, Balu D, Morgan TE, LaDu MJ, Finch CE, et al. , 2019 May 21. APOE genotype and sex affect microglial interactions with plaques in Alzheimer's disease mice. *Acta Neuropathol Commun* 7 (1), 82. [PubMed: 31113487]
- Tai LM, Bilousova T, Jungbauer L, Roeske SK, Youmans KL, Yu C, et al. , 2013 Feb 22. Levels of soluble apolipoprotein E/amyloid- β (A β) complex are reduced and oligomeric A β increased with APOE4 and Alzheimer disease in a transgenic mouse model and human samples. *J. Biol. Chem* 288 (8), 5914–5926. [PubMed: 23293020]
- Tai LM, Koster KP, Luo J, Lee SH, Wang YT, Collins NC, et al. , 2014 Oct 31. Amyloid- β pathology and APOE genotype modulate retinoid X receptor agonist activity in vivo. *J. Biol. Chem* 289 (44), 30538–30555. [PubMed: 25217640]
- Tai LM, Balu D, Avila-Munoz E, Abdullah L, Thomas R, Collins N, et al. , 2017 Sep. EFAD transgenic mice as a human APOE relevant preclinical model of Alzheimer's disease. *J. Lipid Res* 58 (9), 1733–1755. [PubMed: 28389477]

- Tangpong J, Cole MP, Sultana R, Joshi G, Estus S, Vore M, et al. , 2006 Jul. Adriamycin-induced, TNF-alpha-mediated central nervous system toxicity. *Neurobiol. Dis* 23 (1), 127–139. [PubMed: 16697651]
- Ungar L, Altmann A, Greicius MD, 2014 Jun. Apolipoprotein E, gender, and Alzheimer's disease: an overlooked, but potent and promising interaction. *Brain Imaging Behav* 8 (2), 262–273. [PubMed: 24293121]
- Vinters HV, 2015. Emerging concepts in Alzheimer's disease. *Annu. Rev. Pathol* 10, 291–319. [PubMed: 25387055]
- Ward A, Crean S, Mercaldi CJ, Collins JM, Boyd D, Cook MN, et al. , 2012. Prevalence of apolipoprotein E4 genotype and homozygotes (APOE e4/4) among patients diagnosed with Alzheimer's disease: a systematic review and meta-analysis. *Neuroepidemiology* 38 (1), 1–17. [PubMed: 22179327]
- Williams T, Ruiz AJ, Ruiz AM, Vo Q, Tsering W, Xu G, et al. , 2022 Apr 19. Impact of APOE genotype on prion-type propagation of tauopathy. *Acta Neuropathol Commun* 10 (1), 57. [PubMed: 35440098]
- Yang FN, Bronshteyn M, Flowers SA, Dawson M, Kumar P, Rebeck GW, et al. , 2021 Apr 1. Low CD4+ cell count nadir exacerbates the impacts of APOE e4 on functional connectivity and memory in adults with HIV. *AIDS* 35 (5), 727–736. [PubMed: 33587445]
- Yarchoan M, James BD, Shah RC, Arvanitakis Z, Wilson RS, Schneider J, et al. , 2017. Association of Cancer History with Alzheimer's disease dementia and neuropathology. *J. Alzheimers Dis* 56 (2), 699–706. [PubMed: 28035936]
- Youmans KL, Tai LM, Nwabuisi-Heath E, Jungbauer L, Kanekiyo T, Gan M, et al. , 2012 Dec 7. APOE4-specific changes in A β accumulation in a new transgenic mouse model of Alzheimer disease. *J. Biol. Chem* 287 (50), 41774–41786. [PubMed: 23060451]
- Youmans KL, Tai LM, Kanekiyo T, Stine WB, Michon SC, Nwabuisi-Heath E, et al. , 2012 Mar. Intraneuronal A β detection in 5xFAD mice by a new A β -specific antibody. *Mol. Neurodegener* 16 (7), 8.
- Zetterberg H, Bendlin BB, 2021 Jan. Biomarkers for Alzheimer's disease-preparing for a new era of disease-modifying therapies. *Mol. Psychiatry* 26 (1), 296–308. [PubMed: 32251378]
- Zhao N, Attrebi ON, Ren Y, Qiao W, Sonustun B, Martens YA, et al. , 2020 Feb 5. APOE4 exacerbates α -synuclein pathology and related toxicity independent of amyloid. *Sci. Transl. Med* 12 (529), eaay1809.
- Zhu Y, Nwabuisi-Heath E, Dumanis SB, Tai LM, Yu C, Rebeck GW, et al. , 2012 Apr. APOE genotype alters glial activation and loss of synaptic markers in mice. *Glia* 60 (4), 559–569. [PubMed: 22228589]

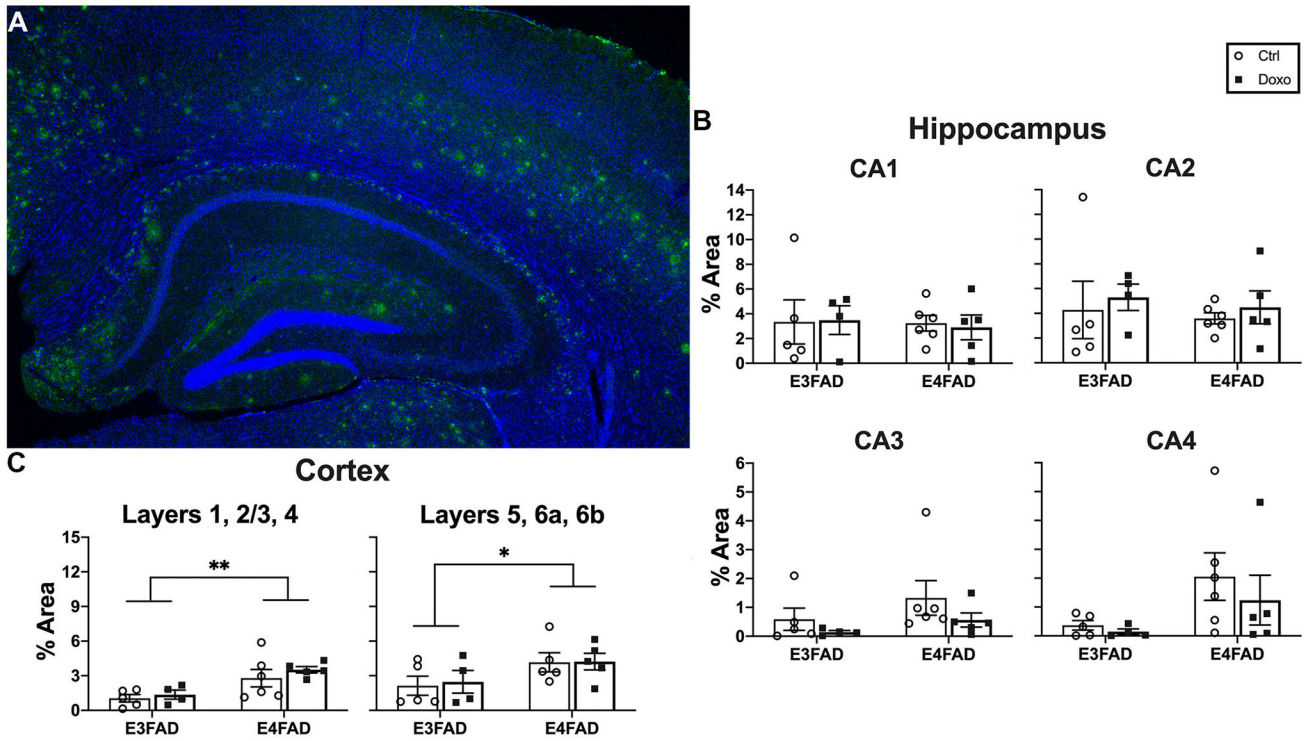


Fig. 1. Coronal sections from E3FAD and E4FAD mice treated with control (Ctrl) or doxorubicin (Doxo) were stained with 6E10 antibodies, against A β /APP. Images were captured at 10 \times magnification in \sim 3 slices per brain; (A) representative image at 2.5 \times of areas analyzed for 6E10 immunostain (green) and DAPI stain (blue). (B–C) bar graphs represent the mean \pm SEM, $n = 5$ –6 animals per group, analysis of percent area coverage of positive plaques within 1, 2/3, 4, 5, 6a, and 6b layers of the cortex and CA1, CA2, CA3, CA4 of the hippocampus. A two-way ANOVA Sidak’s multiple comparison test was used to assess outcome measures from genotype and treatment (* $p = 0.039$, ** $p = 0.0022$).

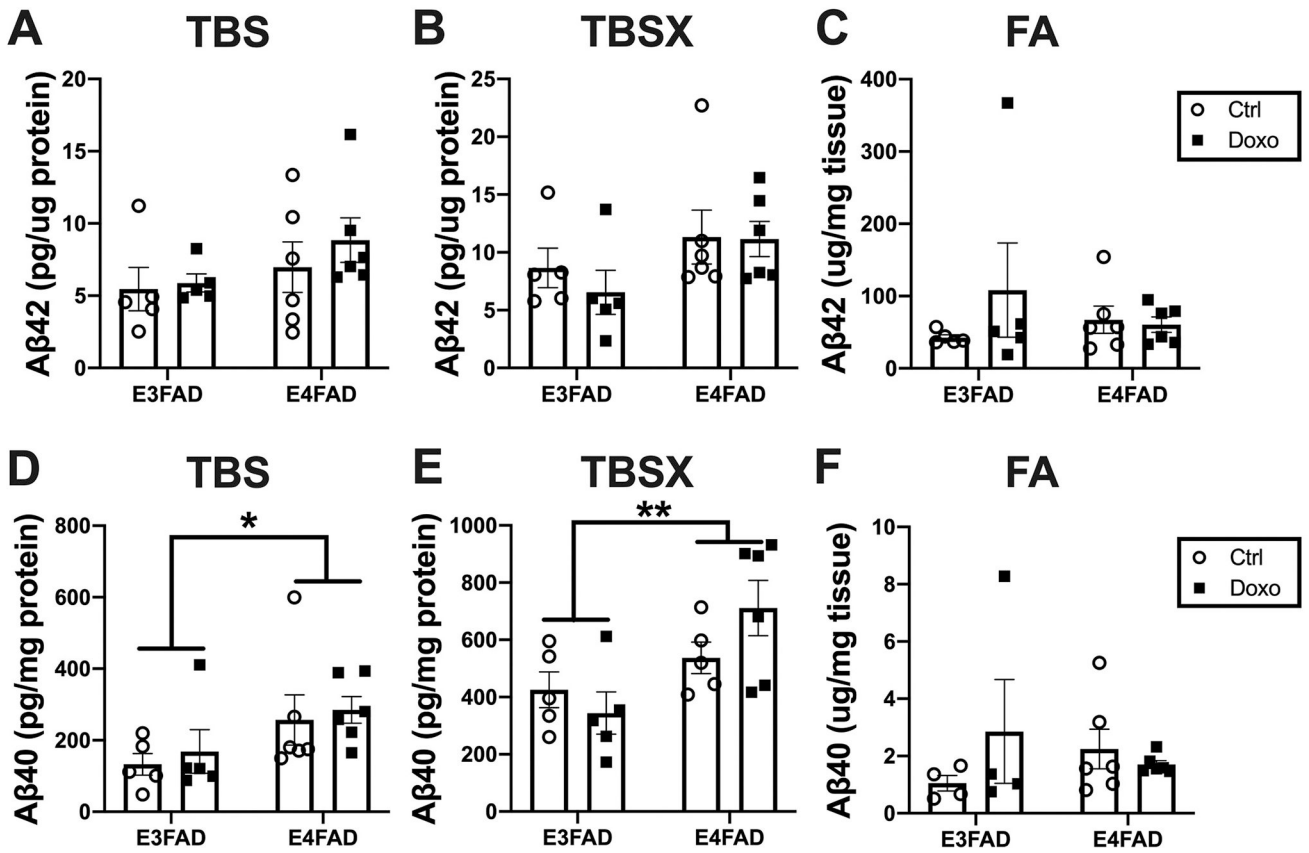


Fig. 2. Tris-Buffered Saline (TBS), Tris-Buffered Saline with 1% Triton-X (TBS-X), and Formic Acid (FA) sequential fractions of hippocampal tissue from E3FAD and E4FAD mice, treated with control (Ctrl) or doxorubicin (Doxo), were obtained as described in material and methods. Lysates were assessed by Aβ42 (A-C) or Aβ40 (D-F) ELISA. Aβ levels in TBS and TBS-X were calculated per total protein, while Aβ levels in FA were calculated per total tissue weight. Bar graphs represent the mean ± SEM, *n* = 5–6 animals per group. A two-way ANOVA with Sidak’s multiple comparison test was used to assess outcomes of measures from genotype and treatment (**p* = 0.038, ***p* = 0.0064).

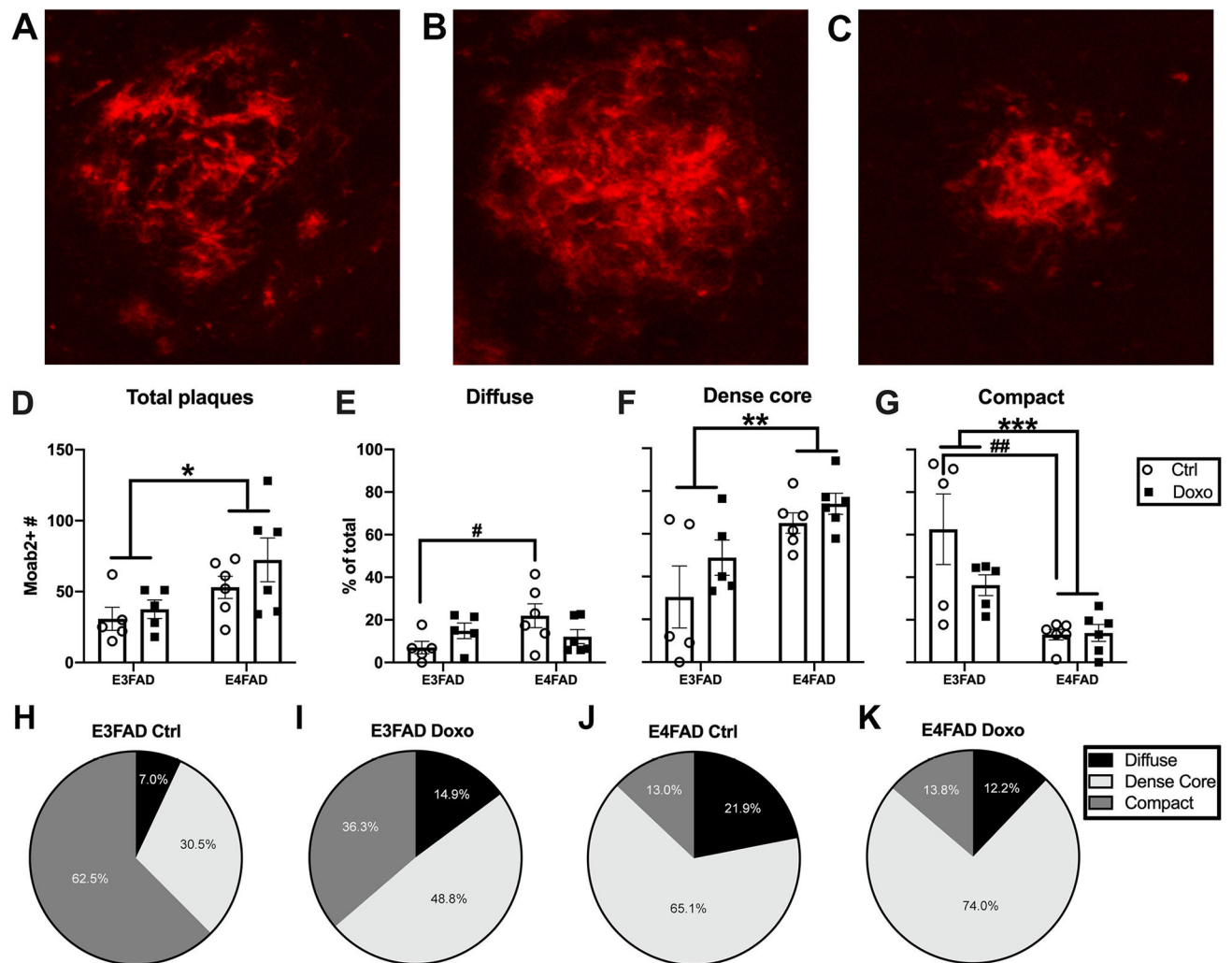


Fig. 3. Coronal sections from E3FAD and E4FAD mice treated with control (Ctrl) or doxorubicin (Doxo) were stained with Moab2 antibodies against A β . Z-stack images of amyloid plaques in the isocortex were captured at 60 \times water immersion magnification using confocal microscopy, ~3 images per ~3 slices from each brain. Plaques were categorized into three morphologies: diffuse (A), dense core (B), and compact (C). Total number of Moab2 positive (Moab2+ #) plaques (D) and percent of the total (% of total) plaques per morphology (E-G) within groups were assessed; (H-K) pie charts of mean percentage of plaque morphology per treatment group. Two-way ANOVAs were used to assess outcome measures of genotype and doxorubicin. Bar graphs represent the mean \pm SEM, $n = 5-6$ animals per group, * represents significant difference of genotype overall (combined treated and control), while # represents significant difference between control groups only (* $p = 0.016$, ** $p = 0.0023$, *** $p = 0.0004$, # $p = 0.041$, ## $p = 0.0009$).

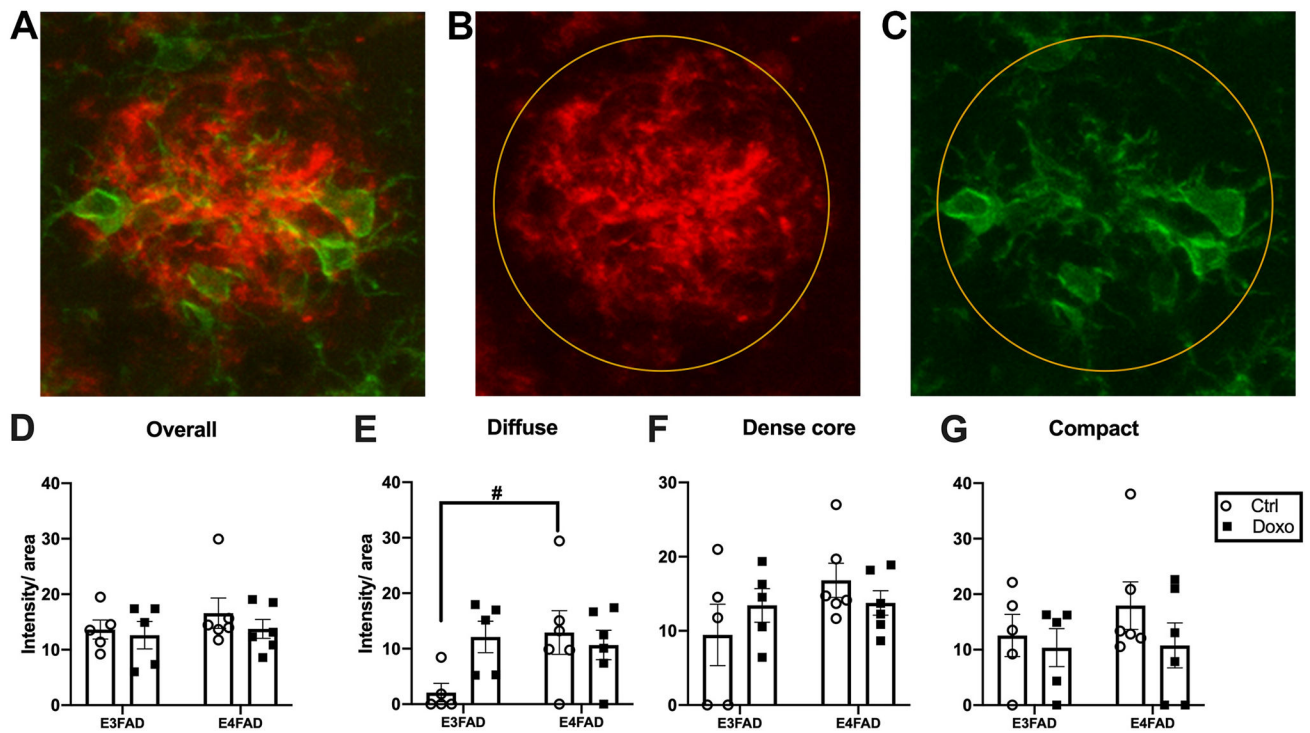


Fig. 4.

Coronal sections from E3FAD and E4FAD mice treated with control (Ctrl) or doxorubicin (Doxo) were co-stained with Moab2 antibodies for A β and Iba1 antibodies for activated microglia. Z-stack images of amyloid plaques in the isocortex were captured at 60 \times water immersion magnification using confocal microscopy, \sim 3 images per \sim 3 slices from each brain. (A) representative 2-dimensional composite images microglia (green) and amyloid plaques (red), (B) circular ROI domains used assess plaque area, (C) and associated microglia activation within the plaque area. Microglia mean intensity per plaque area was assessed per treatment group (D) then evaluated within the plaque types (E-G). Two-way ANOVAs were used to assess outcome measures from genotype and doxorubicin treatment. Bar graphs represent the mean \pm SEM, $n = 5-6$ animals per group, # represents significant difference in microglia response to diffuse plaques between control groups ($\#p = 0.040$).

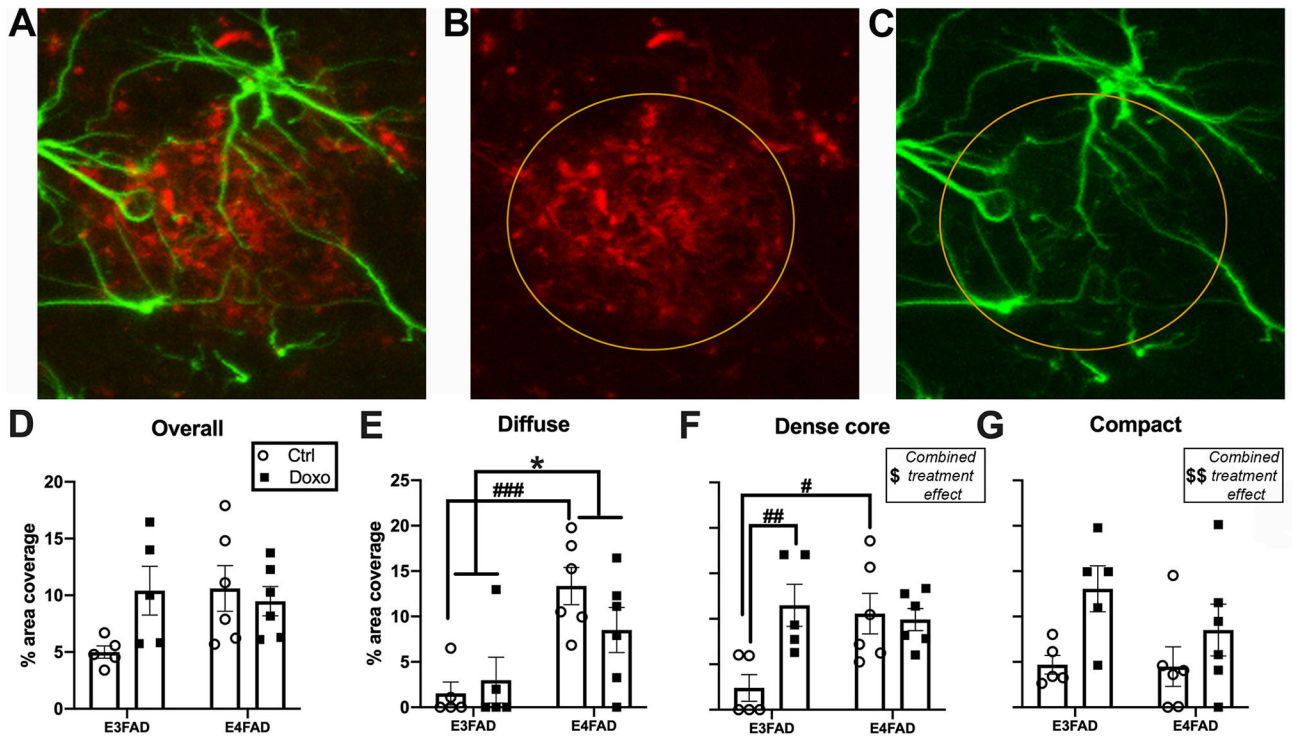


Fig. 5. Coronal sections from E3FAD and E4FAD mice treated with control (Ctrl) or doxorubicin (Doxo) were co-stained with Moab2 antibodies for A β and GFAP antibodies for astrocytes. Z-stack images of amyloid plaques in the isocortex were captured at 60 \times water immersion magnification using confocal microscopy, ~3 images per ~3 slices from each brain. (A) representative 2-dimensional composite images of astrocytes (green) and amyloid plaques (red), (B) circular ROI domains used to assess plaque area and (C) associated astrocytes. Astrocyte % area coverage per plaque area was assessed per group (D) then divided into plaque morphology categories (E-G). Two-way ANOVAs were used to assess outcome measures from genotype and doxorubicin treatment. Bar graphs represent the mean \pm SEM, n = 5–6 animals per group, \$ and \$\$ represent significant effects of treatment overall (combined genotypes), * represents significant effect of genotype overall (combined treatment groups), # represents significant difference between individual groups ($p = 0.036$, \$\$ $p = 0.016$, * $p = 0.0009$, # $p = 0.013$, ### $p = 0.0081$, ### $p = 0.0025$).